Chapter 5

MEASUREMENT OF BEHAVIORAL UNCERTAINTIES IN MECHANICAL VIBRATION SYSTEMS: A SYMBOLIC DYNAMICS APPROACH*

Shalabh Gupta, Dheeraj Singh, Abhishek Srivastav and Asok Ray
Mechanical Engineering Department, The Pennsylvania State University,
University Park, PA 16802, USA

Abstract

Maturity of engineering and scientific theories in recent decades has facilitated creation of advanced technology of human-engineered complex (e.g., electro-mechanical, transportation, and power generation) systems. A vast majority of these systems are often subjected to mechanical vibration. A possible consequence is performance degradation and structural damage that may eventually lead to widespread catastrophic failures. This chapter presents a recently reported technique of data-driven pattern recognition, called Symbolic Dynamic Filtering (*SDF*), for online detection of slowly evolving anomalies (i.e., deviation from the nominal characteristics) and the associated behaviorial uncertainties. The underlying concept of *SDF* is built upon the principles of Statistical Mechanics, Symbolic Dynamics and Information Theory, where time series data from selected sensor(s) in the fast time scale of the process dynamics are analyzed at discrete epochs in the slow time scale of anomaly evolution. Symbolic dynamic filtering includes preprocessing of time series data using the Hilbert transform. The transformed data is partitioned using the maximum entropy principle to generate the symbol sequences, such that the regions of the data space with more information are partitioned finer and those with sparse information are partitioned coarser. Subsequently, statistical patterns of evolving anomalies are identified from these symbolic sequences through construction of a (probabilistic) finite-state machine that captures the system behavior by means of information compression. The concept of *SDF* has been experimentally validated on a special-purpose computer-controlled multi-degree of freedom mechanical vibration apparatus that is instrumented with two accelerometers for identification of anomalous patterns due to parametric changes.

1.   Introduction

A traditional approach of investigating the properties of modern day human-engineered complex (e.g., electro-mechanical, transportation, and power generation) systems involves development of an analytical model of the underlying process dynamics and identification of its critical parameters. However, such a model-based approach for behavioral analysis of a complex system is often limited due to the presence of several difficulties such as: 1) high dimensionality of the system, 2) underlying non-stationary (possibly chaotic) behavior, 3) nonlinearity, and 4) exogenous disturbances. A vast majority of these systems are often subjected to mechanical vibration, and a major goal is online detection and estimation of behavioral uncertainties due to gradual development of anomalies. (Note: Anomaly in a dynamical system is defined as a deviation of its behavior pattern from the nominal pattern that is viewed as the desired healthy behavior.)

Anomalous behavior can be associated with either parametric or non-parametric changes in the dynamics of a complex system. Parametric changes are usually related to degradation of a single or multiple parameters that are often used to construct the analytical model of the system. For example, a change in the stiffness parameter of the diaphragm of a flexible mechanical coupling between two shafts can lead to misalignments and cause whirling. The whirling phenomenon increases machine vibrations and eventually lead to failures of the bearing, coupling and other components of the system. Therefore, the changes in the dynamics of the system can be directly associated to the changes in system model parameters. The other possible changes that can occur in a system are termed as non-parametric changes that are difficult to measure, identify and model, and a direct relation of their effects on the performance variables may not be explicitly known. These non-parametric changes also affect the response of system's observables. However, the exact interpretation and quantification of these changes might not be feasible because of the lack of knowledge of the underlying physics. For example, the growth of fatigue damage in polycrystalline alloys occurs due to small microstructural changes during the crack initiation period. This be represented as a non-parametric change, which is often difficult to model. Therefore, time series data of sensors (e.g., ultrasonic flaw detectors) are used to detect these small microstructural changes during early stages of fatigue damage evolution [1][2].

The above discussion evinces that sole reliance on model-based analysis for pattern recognition is infeasible because of the difficulties in achieving requisite modeling accuracy and in determining the accurate initial conditions with the available computational resources. In general, the analytical models of complex systems could be very sensitive to the initial and boundary conditions and also on certain critical system parameters. Small deviations in these parameters may produce large variations in the evolution of the system for (apparently) identical operating conditions and can possibly lead to chaos [3]. Furthermore, in real-time applications, the analysis of these models becomes computationally very expensive for high-dimensional systems. As such, the problem is tackled using an alterna-

tive approach of observation-based estimation of the underlying process dynamics and the relevant system parameters.

The observed behavioral pattern changes (i.e., parametric or non-parametric) are often indicatives of hidden anomalies that may degrade safety and reliability of mechanical vibration systems. Accurate prediction and quantification of these anomalies could be infeasible due to lack of relevant information or inadequacy of analytical tools that extract such information. This problem is often circumvented by conservative enforcement of large safety factors, which could increase the life of operating machinery but leads to higher costs. A possible solution to reduction of overly conservative safety factors is to have frequent inspections that also turns out to be expensive and time-consuming if maintenance actions are taken based on fixed usage intervals. From these perspectives, it is logical to have online identification of anomalous patterns, which would allow continual re-evaluation of the system and enhance inherent protection against unforeseen impending failures. The online identification of parameters also reduces the frequency of inspections, i.e., increases the mean time between major maintenance actions. Furthermore, early detection of anomalies and identification of incipient fault patterns are essential for prognosis of forthcoming widespread failures to avert colossal loss of expensive equipment and human life [4].

In view of the above discussion, the analysis of time series data from available sensors is needed for real-time pattern recognition. While there exist many reported techniques (e.g., particle filtering [5][6]) for combined model-based and data-driven pattern recognition, the real-time execution of such tools is an open research issue. As such, this chapter addresses the problem of real-time information extraction using a data-driven pattern recognition method called Symbolic Dynamic Filtering (SDF) that has been presented for anomaly detection and estimation of the critical parameters of the system. SDF is an information-theoretic pattern recognition tool that is built upon a fixed-structure, fixed-order Markov chain, called the *D-Markov machine* [7][8].

The theme of pattern recognition and anomaly detection, formulated in this chapter, is built upon the concepts of *Symbolic Dynamics* [9][10], *Finite State Automata* [11], *Information Theory* and *Statistical Mechanics* [12][13] as a means to qualitatively describe the dynamical behavior in terms of symbol sequences [14] [15]. The core concept of SDF is based on appropriate phase-space partitioning of the dynamical system to obtain symbol sequences [16]. Alternatively, symbol sequences are generated from time series data. The loss of information is minimized by using the concept of *maximized entropy partitioning* [17]. The chapter has adopted the method of Hilbert transform of the data before partitioning for symbol sequence generation [7] [17][18]. Statistical patterns in symbolic sequences are identified through construction of a (probabilistic) finite-state machine [7][11]. For anomaly detection, it suffices that a detectable change in the pattern represents a deviation of the nominal pattern from an anomalous one. The concept of SDF for parameter identification has been experimentally validated on a special-purpose computer-controlled multi-degree of freedom mechanical vibration apparatus. This apparatus is instrumented with two accelerometers that measure the response of the system for a parametric change

that is caused due to the movement of a mass block from its nominal position.

This chapter is organized in five sections. Section 1. provides the background and motivation for data-driven pattern recognition for anomaly detection. Section 2. formulates the problem of anomaly detection in mechanical vibration systems using the notion of two-time-scales. Section 3. provides a brief overview of symbolic dynamic filtering for time series data analysis and pattern recognition. Section 4. presents the description of a multi-degree of freedom mechanical vibration apparatus that is equipped with accelerometers for measuring the vibration data. Section 5. presents experimental results of the mechanical vibration apparatus to demonstrate the efficacy of SDF-based pattern recognition and anomaly detection technique. Section 6. summarizes and concludes the chapter with recommendations for future research.

2. Problem Formulation

This section formulates the problem of anomaly detection in complex systems (e.g., the mechanical vibration systems) using the concepts of symbolic dynamic filtering (SDF). In the current chapter the problem of anomaly detection refers to detection of parametric changes in mechanical vibration systems. The underlying features and essential details of SDF [7][13] are presented in the next section.

Anomaly detection using SDF is formulated as a two-time-scale problem as explained below.

- The *fast scale* is related to the response time of process dynamics. Over the span of a given time series data sequence, the behavioral statistics of the system are assumed to remain invariant, i.e., the process is assumed to have statistically stationary dynamics at the fast scale. In other words, statistical variations in the internal dynamics of the system are assumed to be negligible on the fast time scale.

- The *slow scale* is related to the time span over which the process may exhibit non-stationary dynamics due to (possible) evolution of anomalies. Thus, an observable non-stationary behavior can be associated with anomalies evolving at a slow scale.

A pictorial view of the two time scales is presented in Figure 1. In general, a long time span in the fast scale is a tiny (i.e., several orders of magnitude smaller) interval in the slow scale. For example, fatigue damage evolves on a slow scale, possibly in the order of months or years, in machinery structures that are operated in the fast scale approximately in the order of seconds or minutes. Hence, the behavior pattern of fatigue damage is essentially invariant on the fast scale. Nevertheless, the notion of fast and slow scales is dependent on the specific application, loading conditions and operating environment. As such, from the perspective of anomaly detection, sensor data acquisition is done on the fast scale at different slow time epochs.
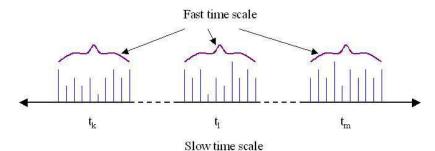
Figure 1. Pictorial view of the two time scales: 1) *slow time scale* where anomalies evolve and 2) *fast time scale* where data acquisition is done.

Anomalies (e.g., microscopic fatigue damage) in complex systems such as rotating machinery, civil infrastructures and aviation systems are often observed as changes in the behavioral characteristics of the system. These changes can be monitored using time-series data (e.g. vibration) of self-excited systems [19] or from the response to an external stimuli [20]. Vibration-based fault detection and identification has been reported in recent literature for a variety of applications such as gear-box [21][22], bearings [23], rotating machines [24], and mechanical structures [25][26]. Anomaly detection using vibration characteristics is a useful method as it partially alleviates the need for a prior knowledge of an analytical model of the system. However, time series analysis of the vibration data for detecting embedded fault signatures in the system is a challenging task. Several methods of feature extraction and time-series analysis can be used to this effect. Methods such as Fourier and wavelet transforms [27], Hilbert-Huang transform [28], Hidden Markov Modeling [29], Artificial Neural Network (ANN) [30], and fuzzy inference systems [31] have been used for analysis of vibration signals. Often the evolution of anomalies leads to non-linear (possibly chaotic [32]) dynamics which may be difficult to model or approximate. Small changes in the system dynamical behavior may not be directly discernable using frequency spectrum or modal analysis and present the need for advanced signal processing and pattern recognition methods. These issues have motivated the study of anomaly detection in vibration systems from the perspectives of dynamical systems [33][34].

Symbolic Dynamic Filtering (SDF) for anomaly detection presented in this chapter has been experimentally validated for real-time execution in different applications, such as electronic circuits [35], mechanical structures for fatigue damage monitoring [1][36][37][2][38][40], gasification systems for detection of refractory degradation [39], and rotating machinery for detection of shaft misalignment [41]. Furthermore, it has been shown that SDF yields superior performance in terms of early detection of anomalies and robustness to measurement noise by comparison with other existing techniques such as Principal Component Analysis (PCA) and Artificial Neural Networks (ANN) [35][1].

The task of anomaly detection is to enable both (a) *diagnosis* - detection and extraction of anomalous behavior, and (b) *prognosis*, tracking failure precursors leading to faults. Therefore, the anomaly detection problem is partitioned into two problems [7]: (i) *forward*
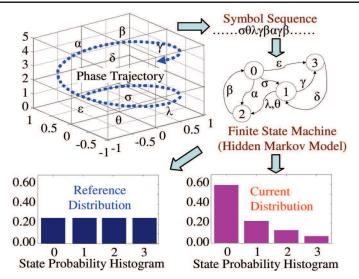
Figure 2. Conceptual view of symbolic dynamic filtering.

problem of pattern recognition for monitoring the evolution of system dynamics by (offline) analysis of the anomalous behavior, relative to the nominal behavior; and (ii) *inverse problem of pattern identification* for (online) estimation of parametric or non-parametric changes based on the knowledge assimilated in the forward problem and the observed time series data of quasi-stationary process response. The inverse problem could be ill-posed or have no unique solution. That is, it may not always be possible to identify a unique anomaly pattern based on the observed behavior of the dynamical system. Nevertheless, the feasible range of parameter variation estimates can be narrowed down from the intersection of the information generated from inverse images of the responses under several stimuli. The algorithms of SDF can be implemented to solve both these problems; however, the current chapter has addressed only the forward problem of anomaly detection and the inverse problem of parameter estimation is reported as an area of future work.

3.   Review of Symbolic Dynamic Filtering (SDF)

This section presents the underlying concepts and salient features of SDF for anomaly detection in complex dynamical systems. While the details are reported in previous publications [7][8][13][17][42], the essential concepts of space partitioning, symbol sequence generation, construction of a finite-state machine from the generated symbol sequence and pattern recognition are consolidated here and succinctly described for self-sufficiency and completeness of the chapter.

3.1.   Symbolic Dynamics and Encoding

This subsection briefly describes the concepts of *Symbolic Dynamics* for:

1. Encoding nonlinear system dynamics from observed time series data for generation of symbol sequences, and

2. Construction of a probabilistic finite state machine ($PFSM$) from the symbol sequence for generation of pattern vectors as representation of the dynamical system's characteristics.

The continuously-varying finite-dimensional model of a dynamical system is usually formulated in the setting of an initial value problem as:

$$\frac{d\mathbf{x}(t)}{dt} = f(\mathbf{x}(t), \theta(\tau)); \; \mathbf{x}(0) = \mathbf{x}_0, \tag{1}$$

where $t \in [0, \infty)$ denotes the (fast-scale) time; $\mathbf{x} \in \mathbb{R}^n$ is the state vector in the phase space; and $\theta \in \mathbb{R}^\ell$ is the (possibly anomalous) parameter vector varying in (slow-scale) time τ. The gradual change in the parameter vector $\theta \in \mathbb{R}^\ell$ due to possible evolution of anomalies on the slow time scale can alter the system dynamics and hence change the state trajectory.

Let $\Omega \subset \mathbb{R}^n$ be a compact (i.e., closed and bounded) region, within which the trajectory of the dynamical system, governed by Eq. (1), is circumscribed as illustrated in Fig. 2. The region Ω is partitioned as $\{\Phi_0, \cdots, \Phi_{|\Sigma|-1}\}$ consisting of $|\Sigma|$ mutually exclusive (i.e., $\Phi_j \cap \Phi_k = \emptyset \; \forall j \neq k$), and exhaustive (i.e., $\bigcup_{j=0}^{|\Sigma|-1} \Phi_j = \Omega$) cells, where Σ is the *symbol alphabet* that labels the partition cells. A trajectory of the dynamical system is described by the discrete time series data as: $\{\mathbf{x}_0, \mathbf{x}_1, \mathbf{x}_2, \cdots\}$, where each $\mathbf{x}_i \in \Omega$. The trajectory passes through or touches one of the cells of the partition; accordingly the corresponding symbol is assigned to each point $\mathbf{x}_i$ of the trajectory as defined by the mapping $\mathcal{M} : \Omega \to \Sigma$. Therefore, a sequence of symbols is generated from the trajectory starting from an initial state $\mathbf{x}_0 \in \Omega$, such that:

$$\mathbf{x}_0 \rightarrowtail s_0 s_1 s_2 \ldots s_j \ldots \tag{2}$$

where $s_k \triangleq \mathcal{M}(\mathbf{x}_k)$ is the symbol generated at the (fast scale) instant k. The symbols $s_k, \; k = 0, 1, \ldots$ are identified by an index set $\mathcal{I} : \mathbb{Z} \to \{0, 1, 2, \ldots |\Sigma|-1\}$, i.e., $\mathcal{I}(k) = i_k$ and $s_k = \sigma_{i_k}$ where $\sigma_{i_k} \in \Sigma$. Equivalently, Eq. (2) is expressed as:

$$\mathbf{x}_0 \rightarrowtail \sigma_{i_0} \sigma_{i_1} \sigma_{i_2} \ldots \sigma_{i_j} \ldots \tag{3}$$

The mapping in Eq. (2) and Eq. (3) is called *Symbolic Dynamics* as it attributes a legal (i.e., physically admissible) symbol sequence to the system dynamics starting from an initial state. The partition is called a generating partition of the phase space Ω if every legal (i.e., physically admissible) symbol sequence uniquely determines a specific initial condition $\mathbf{x}_0$. In other words, every (semi-infinite) symbol sequence uniquely identifies one continuous space orbit [15].

Symbolic dynamics may also be viewed as coarse graining of the phase space, which is subjected to (possible) loss of information resulting from granular imprecision of partitioning boxes. However, the essential robust features (e.g., periodicity and chaotic behavior

of an orbit) are expected to be preserved in the symbol sequences through an appropriate partitioning of the phase space [14].

Figure 2 pictorially elucidates the concepts of partitioning a finite region of the phase space and the mapping from the partitioned space into the symbol alphabet, where the symbols are indicated by Greek letters (e.g., $\alpha, \beta, \gamma, \delta, \cdots$). This represents a spatial and temporal discretization of the system dynamics defined by the trajectories. Figure 2 also shows conversion of the symbol sequence into a finite-state machine and generation of the state probability vectors at the current and the reference conditions. The states of the finite state machine and the histograms in Fig. 2 are indicated by numerics (i.e., 1, 2, 3 and 4); the necessary details are provided later in Section 3.3.. Although the theory of phase-space partitioning is well developed for one-dimensional mappings [15], very few results are known for two and higher dimensional systems. Furthermore, the state trajectory of the system variables may be unknown in case of systems for which a model as in Eq. (1) is not known or is difficult to obtain. As such, as an alternative, the time series data set of selected observable outputs can be used for symbolic dynamic encoding (see Section 3.2. for further details).

3.2.   Analytic Signal Space Partitioning

As described earlier, a crucial step in symbolic dynamic filtering (SDF) is partitioning of the phase space for symbol sequence generation [10]. Several partitioning techniques have been reported in literature for symbol generation [43][16], primarily based on symbolic false nearest neighbors ($SFNN$). These techniques rely on partitioning the phase space and may become cumbersome and extremely computation-intensive if the dimension of the phase space is large. Moreover, if the time series data is noise-corrupted, then the symbolic false neighbors would rapidly grow in number and require a large symbol alphabet to capture the pertinent information on the system dynamics. Therefore, symbolic sequences as representations of the system dynamics should be generated by alternative methods because phase-space partitioning might prove to be a difficult task in the case of high dimensions and presence of noise.

The wavelet-space partitioning (WSP) [7][17] was introduced as an alternative to $SFNN$ partitioning. The wavelet coefficients at selected scale(s) are stacked back to back to transform the 2-dimensional scale-shift wavelet domain into a one-dimensional domain. The resulting scale-series data sequence is converted to a sequence of symbols by *maximum entropy partitioning* [17]. The wavelet transform [44] largely alleviates the above mentioned shortcomings of $SFNN$ partitioning and is particularly effective with noisy data from high-dimensional dynamical systems [17].

Although WSP is significantly computationally faster than $SFNN$ partitioning and is suitable for real-time applications, WSP has several shortcomings as follows:

- *Selection of an appropriate wavelet basis function*: This selection is made such that the shape of the basis function closely matches that of the signal, which may vary

with the window size. Apparently, there is no precise way of selecting a wavelet basis that is "best" for partitioning.

- *Identification of scales for generation of wavelet coefficients*: Scales are identified from the center frequency (that is based on inspection of the power spectral density of the Fourier transform) and the selected wavelet basis.

- *Dimension reduction of the scale-shift wavelet domain*: This reduction to a one-dimensional domain of *scale-series* sequences is non-unique and may not be a "best" way.

Therefore, another alternative to the existing partitioning methods has been recently proposed, called analytic signal space partitioning ($ASSP$) [18]. Although $ASSP$ is not aimed to be a generating partition, it is designed with the goal of satisfying the important property of a generating partition: *The inverse image of a small neighborhood in the symbol space is a small neighborhood in the data space*, except possibly in the vicinity of partition boundaries. The underlying concept of $ASSP$ partitioning is built upon Hilbert transform of the observed real-valued data sequence into the corresponding complex-valued analytic signal [45] as explained below.

Let $x(t)$ be a real-valued function whose domain is the real field $\mathbb{R} = (-\infty, +\infty)$. Then, Hilbert transform [18] of $x(t)$ is defined as:

$$\widetilde{x}(t) = \mathcal{H}[x](t) = \frac{1}{\pi} \int_{\mathbb{R}} \frac{x(\tau)}{t - \tau} d\tau \tag{4}$$

That is, $\widetilde{x}(t)$ is the convolution of $x(t)$ with $\frac{1}{\pi t}$ over $\mathbb{R}$, which is represented in the Fourier domain as:

$$\mathcal{F}[\widetilde{x}](\xi) = -i\, sgn(\xi)\, \mathcal{F}[x](\xi) \tag{5}$$

where $sgn(\xi) = \begin{cases} +1 & \text{if } \xi > 0 \\ -1 & \text{if } \xi < 0 \end{cases}$

Given the Hilbert transform of a real-valued signal $x(t)$, the corresponding complex-valued analytic signal is defined as:

$$\mathcal{A}[x](t) = x(t) + i\, \widetilde{x}(t) \tag{6}$$

The construction of Eq. (6) is based on the fact that the values of Fourier transform of a real-valued function at negative frequencies are redundant due to their Hermitian symmetry imposed by the transform. Thus, the phase of the Hilbert transform $\widetilde{x}(t)$ is in quadrature to the phase of $x(t)$. That is, the analytic signal can be expressed as:

$$\mathcal{A}[x](t) = A(t)\, \exp\big(i\, \varphi(t)\big) \tag{7}$$

where $A(t)$ and $\varphi(t)$ are called the instantaneous amplitude and instantaneous phase of $\mathcal{A}[x](t)$, respectively. Vakman [46] has pointed out that the amplitude and phase of an analytic signal satisfy the following three physical properties:

1. *Amplitude Continuity*: A small perturbation in $x(t)$ induces a small change in $A(t)$.

2. *Phase independence of scale*: Scaling $x(t)$ by a constant $c > 0$ has no effects on $\varphi(t)$ and multiplies $A(t)$ by c.

3. *Harmonic correspondence*: A mono-frequency signal (i.e., a pure sinusoid $A_0 cos(\omega_0 t + \varphi_0)$) yields $A(t) = A_0$ and $\varphi(t) = \omega_0 t + \varphi_0$ for all t.

Thus, for a mono-frequency signal, which is embedded in a 2-dimensional state space, a direct parallel can be drawn between the phase plot and the Hilbert transform plot. The procedure for $ASSP$ is formulated next.

Let the observed signal be available as a real-valued time series of N data points. Upon Hilbert transformation of this data sequence, a pseudo-phase plot is constructed from the resulting analytic signal by a bijective mapping of the complex field onto $\mathbb{R}^2$, i.e., by plotting the real and the imaginary parts of the analytic signal on the x_1 and x_2 axes, respectively. It is important to note that the pseudo-phase space is always two-dimensional, whereas the phase space of the dynamical system is a representation of the n-dimensional manifold, where n could be an arbitrarily large positive integer.

The time-dependent analytic signal in Eq. (6) is now represented as a (one-dimensional) trajectory in the two-dimensional pseudo-phase space. Let Ξ be a compact region in the pseudo-phase space, which encloses the trajectory. The objective is to partition Ξ into finitely many mutually exclusive and exhaustive segments, where each segment is labeled with a symbol or letter. The segments are conveniently determined by the magnitude and phase of the analytic signal as well as based on the density of data points in these segments. That is, if the magnitude and phase of a data point of the analytic signal lies within a segment or on its boundary, then the data point is labeled with the corresponding symbol. Thus, a symbol sequence is derived from the (complex-valued) sequence of the analytic signal. The set of (finitely many) symbols is called the alphabet Σ.

One possible way of partitioning Ξ is to divide the magnitude and phase of the time-dependent analytic signal in Eq. (6) into uniformly spaced segments between their maximum and minimum values, respectively. This is called the uniform partitioning. An alternative method, known as the maximum entropy partitioning [17], maximizes the entropy of the partition that is characterized by the alphabet size $|\Sigma|$, thereby imposing a uniform probability distribution on the symbols. The maximum entropy partitioning is generated by maximizing the Shannon entropy [47], which is defined as:

$$S = - \sum_{i=0}^{|\Sigma|-1} p_i \, log(p_i) \tag{8}$$

where p_i is the probability of a data point to be in the ith partition segment. In this partitioning, regions with rich information are partitioned into finer segments than those with sparse information. Computationally the maximum entropy partition can be obtained by sorting the data sequence in an ascending order. This sorted data sequence is then partitioned into

$|\Sigma|$ equal segments of length $\lfloor \frac{N}{|\Sigma|} \rfloor$, where N is the length of the data sequence and $\lfloor x \rfloor$ is the greatest integer less than or equal to x. Each of these segments is assigned a symbol and all data points in a given segment are assigned the corresponding symbol.

The magnitude and phase of the analytic signal in Eq. (6) are partitioned separately according to either uniform partitioning, maximum entropy partitioning or any other type of partitioning; the type of partitioning may depend on the characteristics of the physical process. In essence, each point in the data set is represented by a pair of symbols – one belonging to the alphabet Σ_R based on the magnitude (i.e., in the radial direction) and the other belonging to the alphabet Σ_A based on the phase (i.e., in the angular direction). The analytic signal is converted into a one dimensional symbol sequence by associating each pair of symbols into a symbol from a new alphabet Σ as:

$$\Sigma \triangleq \big\{(\sigma_i, \sigma_j) : \ \sigma_i \in \Sigma_R, \ \sigma_j \in \Sigma_A\big\} \text{ and } |\Sigma| = |\Sigma_R| \cdot |\Sigma_A|$$

3.3. Probabilistic Finite State Machine ($PFSM$) and Pattern Recognition

Once the symbol sequence is obtained, the next step is the construction of a Probabilistic Finite State Machine ($PFSM$) and calculation of the respective state probability vector as depicted in the lower part of Fig. 2 by the histograms. The partitioning is performed at the reference condition.

A $PFSM$ is then constructed, where the states of the machine are defined corresponding to a given *alphabet* set Σ and window length D. The alphabet size $|\Sigma|$ is the total number of partition segments while the window length D is the length of consecutive symbol words [7], which are chosen as all possible words of length D from the symbol sequence. Each state belongs to an equivalence class of symbol words of length D, which is characterized by a word of length D at the leading edge. Therefore, the number n of such equivalence classes (i.e., states) is less than or equal to the total permutations of the alphabet symbols within words of length D. That is, $n \leq |\Sigma|^D$; some of the states may be forbidden, i.e., these states have zero probability of occurrence. For example, if $\Sigma = \{\alpha, \beta\}$, i.e., $|\Sigma| = 2$ and if $D = 2$, then the number of states is $n \leq |\Sigma|^D = 4$; and the possible states are words of length $D = 2$, i.e., $\alpha\alpha, \alpha\beta, \beta\alpha,$ and $\beta\beta$, as shown in Fig. 3.
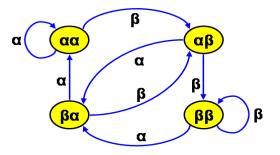

Figure 3. Example of Finite State Machine with D=2 and $\Sigma = \{\alpha, \beta\}$

The choice of $|\Sigma|$ and D depends on specific applications and the noise level in the time series data as well as on the available computation power and memory availability. As stated earlier, a large *alphabet* may be noise-sensitive and a small alphabet could miss the details of signal dynamics. Similarly, while a larger value of D is more sensitive to signal distortion, it would create a much larger number of states requiring more computation power and increased length of the data sets. In the results section of this chapter, the analysis of time series data sets is done using the window length equal to $D=1$; consequently, the set of states Q is equivalent to the symbol alphabet Σ. With the selection of the parameters $D=1$ and $|\Sigma|=8$, the $PFSM$ has $n = 8$ states. With this choice of parameters, the SDF algorithm is shown to be capable of detection of parametric changes in the mechanical system. However, other applications such as two-dimensional image processing, may require larger values of the parameter D and hence possibly larger number of states in the $PFSM$.

Using the symbol sequence generated from the time series data, the state machine is constructed on the principle of sliding block codes [9]. The window of length D on a symbol sequence is shifted to the right by one symbol, such that it retains the most recent $(D\text{-}1)$ symbols of the previous state and appends it with the new symbol at the extreme right. The symbolic permutation in the current window gives rise to a new state. The $PFSM$ constructed in this fashion is called the D-Markov machine [7], because of its Markov properties.

Definition 3..1 *A symbolic stationary process is called D-Markov if the probability of the next symbol depends only on the previous D symbols, i.e., $P\left(s_j|s_{j-1}....s_{j-D}s_{j-D-1}....\right) = P\left(s_j|s_{j-1}....s_{j-D}\right)$.*

The finite state machine constructed above has D-Markov properties because the probability of occurrence of symbol $\sigma \in \Sigma$ on a particular state depends only on the configuration of that state, i.e., the previous D symbols. The states of the machine are marked with the corresponding symbolic word permutation and the edges joining the states indicate the occurrence of a symbol σ. The occurrence of a symbol at a state may keep the machine in the same state or move it to a new state.

Definition 3..2 *Let Ξ be the set of all states of the finite state machine. Then, the probability of occurrence of symbols that cause a transition from state ξ_j to state ξ_k under the mapping $\delta : \Xi \times \Sigma \to \Xi$ is defined as:*

$$\pi_{jk} = P\left(\sigma \in \Sigma \mid \delta(\xi_j, \sigma) \to \xi_k\right); \sum_k \pi_{jk} = 1; \tag{9}$$

Thus, for a D-Markov machine, the irreducible stochastic matrix $\mathbf{\Pi} \equiv [\pi_{ij}]$ describes all transition probabilities between states such that it has at most $|\Sigma|^{D+1}$ nonzero entries. The definition above is equivalent to an alternative representation such that,

$$\pi_{jk} \equiv P(\xi_k|\xi_j) = \frac{P(\xi_j, \xi_k)}{P(\xi_j)} = \frac{P(\sigma_{i_0} \cdots \sigma_{i_{D-1}} \sigma_{i_D})}{P(\sigma_{i_0} \cdots \sigma_{i_{D-1}})} \tag{10}$$

where the corresponding states are denoted by $\xi_j \equiv \sigma_{i_0} \cdots \sigma_{i_{D-1}}$ and $\xi_k \equiv \sigma_{i_1} \cdots \sigma_{i_D}$. This phenomenon is a consequence of the $PFSM$ construction based on the principle of sliding block codes described above, where the occurrence of a new symbol causes a transition to another state or possibly the same state.

For computation of the state transition probabilities from a given symbol sequence at a particular slow time epoch, a D-block (i.e., a window of length D) is moved by counting occurrences of symbol blocks $\sigma_{i_0} \cdots \sigma_{i_{D-1}} \sigma_{i_D}$ and $\sigma_{i_0} \cdots \sigma_{i_{D-1}}$, which are respectively denoted by $N(\sigma_{i_0} \cdots \sigma_{i_{D-1}} \sigma_{i_D})$ and $N(\sigma_{i_0} \cdots \sigma_{i_{D-1}})$. Note that if $N(\sigma_{i_0} \cdots \sigma_{i_{D-1}}) = 0$, then the state $\sigma_{i_0} \cdots \sigma_{i_{D-1}} \in \Xi$ has zero probability of occurrence. For $N(\sigma_{i_0} \cdots \sigma_{i_{D-1}}) \neq 0$, the estimates of the transitions probabilities are then obtained by these frequency counts as follows:

$$\pi_{jk} \approx \frac{N(\sigma_{i_0} \cdots \sigma_{i_{D-1}} \sigma_{i_D})}{N(\sigma_{i_0} \cdots \sigma_{i_{D-1}})} \tag{11}$$

where the criterion for convergence of the estimated π_{jk}, is given in the next subsection 3.4. as a stopping rule for frequency counting.

The symbol sequence generated from the time series data at the reference condition, set as a benchmark, is used to compute the *state transition matrix* $\mathbf{\Pi}$ using Eq. (11). The left eigenvector $\mathbf{q}$ corresponding to the unique unit eigenvalue of the irreducible stochastic matrix $\mathbf{\Pi}$ is the probability vector whose elements are the stationary probabilities of the states belonging to Ξ [7]. Similarly, the state probability vector $\mathbf{p}$ is obtained from time series data at a (possibly) anomalous condition. The partitioning of time series data and the state machine structure should be the same in both cases but the respective state transition matrices could be different. The probability vectors $\mathbf{p}$ and $\mathbf{q}$ are estimates of the respective true probability vectors and are treated as statistical patterns. The terms *probability vector* and *pattern vector* are used interchangeably in the sequel.

Pattern changes may take place in dynamical systems due to accumulation of faults and progression of anomalies. The pattern changes are quantified as deviations from the reference pattern (i.e., the probability distribution at the reference condition). The resulting anomalies (i.e., deviations of the evolving patterns from the reference pattern) are characterized by a scalar-valued function, called *anomaly measure* μ. The anomaly measures are obtained as:

$$\mu \equiv d\left(\mathbf{p}, \mathbf{q}\right) \tag{12}$$

where the $d(\bullet, \bullet)$ is an appropriately defined distance function.

3.4. Stopping Rule for Symbol Sequence Generation

This subsection presents a stopping rule that is necessary to find a lower bound on the length of symbol sequence required for parameter identification of the stochastic matrix $\mathbf{\Pi}$. The stopping rule [8] is based on the properties of irreducible stochastic matrices [48]. The state transition matrix, constructed at the rth iteration (i.e., from a symbol sequence of length r),

is denoted as $\mathbf{\Pi}(r)$ that is an $n \times n$ irreducible stochastic matrix under stationary conditions. Similarly, the state probability vector $\mathbf{p}(r) \equiv [p_1(r) \, p_2(r) \, \cdots \, p_n(r)]$ is obtained as

$$p_i(r) = \frac{r_i}{\sum_{j=1}^{n} r_j} \tag{13}$$

where r_i is the number of D-blocks representing the ith state such that $\left(\sum_{j=1}^{n} r_j \right) + D - 1 = r$ is the total length of the data sequence under symbolization. The stopping rule makes use of the Perron-Frobenius Theorem [48] to establish a relation between the vector $\mathbf{p}(r)$ and the matrix $\mathbf{\Pi}(r)$. Since the matrix $\mathbf{\Pi}(r)$ is stochastic and irreducible, there exists a unique eigenvalue $\lambda = 1$ and the corresponding left eigenvector $\mathbf{p}(r)$ (normalized to unity in the sense of absolute sum). The left eigenvector $\mathbf{p}(r)$ represents the state probability vector, provided that the matrix parameters have converged after a sufficiently large number of iterations. That is, under the hypothetical arbitrarily long sequences, the following condition is assumed to hold.

$$\mathbf{p}(r+1) = \mathbf{p}(r)\mathbf{\Pi}(r) \quad \Rightarrow \quad \mathbf{p}(r) = \mathbf{p}(r)\mathbf{\Pi}(r) \ \text{ as } r \to \infty \tag{14}$$

Following Eq. (13), the absolute error between successive iterations is obtained such that

$$\| \, (\mathbf{p}(r) - \mathbf{p}(r+1)) \, \|_{\infty} = \| \, \mathbf{p}(r) \, (\mathbf{I} - \mathbf{\Pi}(r)) \, \|_{\infty} \leq \frac{1}{r} \tag{15}$$

where $\| \bullet \|_{\infty}$ is the max norm of the finite-dimensional vector $\bullet$.

To calculate the stopping point r_{stop}, a tolerance of η, where $0 < \eta \ll 1$, is specified for the relative error such that:

$$\frac{\| \, (\mathbf{p}(r) - \mathbf{p}(r+1)) \, \|_{\infty}}{\| \, (\mathbf{p}(r)) \, \|_{\infty}} \leq \eta \quad \forall \, r \geq r_{stop} \tag{16}$$

The objective is to obtain the least conservative estimate for r_{stop} such that the dominant elements of the probability vector have smaller relative errors than the remaining elements. Since the minimum possible value of $\| \, (\mathbf{p}(r)) \, \|_{\infty}$ for all r is $\frac{1}{n}$, where n is the dimension of $\mathbf{p}(r)$, the least of most conservative values of the stopping point is obtained from Eqs. (15) and (16) as:

$$r_{stop} \equiv int \left(\frac{n}{\eta} \right) \tag{17}$$

where $int(\bullet)$ is the integer part of the real number $\bullet$.

3.5.   Summary of SDF-based Pattern Recognition

The symbolic dynamic filtering (SDF) method of statistical pattern recognition for anomaly detection is summarized below.

- Acquisition of time series data from appropriate sensor(s) and/or analytical model variables at a reference condition, when the system is assumed to be in the healthy state (i.e., zero anomaly measure)

- Generation of the Hilbert transform coefficients [18]

- Maximum entropy partitioning in the domain of transformed signal at the nominal condition (see Section 3.2.) and generation of the corresponding symbol sequence

- Construction of the D-Markov machine and computation of the state probability vector $\mathbf{q}$ at the reference condition

- Generation of a time series data sequence at another (possibly) anomalous condition and conversion to the wavelet domain to generate the respective symbolic sequence based on the partitioning constructed at the reference condition

- Computation of the corresponding state probability vector $\mathbf{p}$ using the finite state machine constructed at the reference condition

- Computation of scalar *anomaly measure* μ (see Eq. (12)).

Capability of SDF has been demonstrated for anomaly detection at early stages of gradually evolving faults by real-time experimental validation. Application examples include active electronic circuits [35] and fatigue damage monitoring in polycrystalline alloys [1][36][37]. It has been shown that SDF yields superior performance in terms of early detection of anomalies and robustness to measurement noise by comparison with other existing techniques such as Principal Component Analysis (PCA) and Artificial Neural Networks (ANN) [35][1]. In this regard, major advantages of SDF for small anomaly detection are listed below:

- Robustness to measurement noise and spurious signals [17]

- Adaptability to low-resolution sensing due to the coarse graining in space partitions [7]

- Capability for early detection of anomalies because of sensitivity to signal distortion [1] and

- Real-time execution on commercially available inexpensive platforms [35][1].

3.6.   Forward and Inverse problems

As stated earlier in Section 1., the anomaly detection problem is separated into two sub-problems: 1) the *forward (or analysis) problem* and 2) the *inverse (or synthesis) problem. The forward problem* consists of prediction of outcomes, given a priori knowledge of the underlying model parameters. In absence of an existing model this problem requires generation of behavioral patterns of the system evolution through off-line analysis of an ensemble of the observed time series data. On the other hand, *the inverse problem* consists

of estimation of critical parameters characterizing the system under investigation using the actual observations [37]. Inverse problems arise in different engineering disciplines such as geophysics, structural health monitoring, weather forecasting, and astronomy. Inverse problems often become ill-posed and challenging due to the following reasons: (a) high dimensionality of the parameter space under investigation and (b) in absence of a unique solution where change in multiple parameters can lead to the same observations.

In presence of sources of uncertainties, any parameter inference strategy requires estimation of parameter values and also the associated confidence intervals, or the error bounds, to the estimated values. As such, inverse problems are usually solved using the Bayesian methods that allow observation based inference of parameters and provide a probabilistic description of the uncertainty of inferred quantities. A good discussion of inverse problems is presented by Tarantola [49].

In context of anomaly detection, the tasks and solution steps of these two problems as followed in this chapter are discussed below.

3.6.1. Forward Problem

The primary objective of the forward problem is identification of changes in the behavioral patterns of system dynamics due to evolving anomalies on the slow time scale. Specifically, the forward problem aims at detecting the deviations in the statistical patterns in the time series data, generated at different time epochs in the slow time scale, from the nominal behavior pattern. The solution procedure of the forward problem requires the following steps:

F1. Collection of time series data sets (at fast time scale) from the available sensor(s) at different slow time epochs;

F2. Analysis of these data sets using the SDF method as discussed in earlier sections to generate pattern vectors defined by the probability distributions at the corresponding slow time epochs. The profile of anomaly measure is then obtained from the evolution of this pattern vector from the nominal condition;

F3. Generation of a family of such profiles from multiple experiments performed under identical conditions to construct a statistical pattern of anomaly growth. Such a family represents the uncertainty in the evolution of anomalies in dynamical systems due to its stochastic nature. For eg., in case of fatigue damage, the uncertainty arises from the random distribution of microstructural flaws in the body of the component leading to a stochastic behavior [50].

3.6.2. Inverse Problem

The objective of the inverse problem is to infer the anomalies and to provide estimates of system parameters from the observed time series data and system response in real time [37].

Therefore, as a precursor to the solution of the inverse problem, generation of an ensemble of data sets is required during the forward problem for multiple experiments conducted under identical operating conditions. Anomaly estimates can be obtained at any particular instant in a real-time experiment with certain confidence intervals using the information derived from the ensemble of data sets of anomaly evolution generated in the forward problem [7][37]. The solution procedure of the inverse problem requires the following steps:

I1. Collection of time series data sets (in the fast time scale) from the available sensor(s) at different slow time epochs up till the current time epoch in a real-time experiment as in step F1 of the forward problem;

I2. Analysis of these data sets using the SDF method to generate pattern vectors defined by probability distributions at the corresponding slow time epochs. The value of anomaly measure at the current time epoch is then calculated from the evolution of this pattern vector from the nominal condition. The procedure is similar to the step F2 of the forward problem. As such, the information available at any particular instant in a real-time experiment is the value of the anomaly measure calculated at that particular instant;

I3. Detection, identification and estimation of an anomaly (if any) based on the computed anomaly measure and the statistical information derived in step F3 of the forward problem.

The family of anomaly measure profiles is analyzed in the inverse problem to generate the requisite statistical information. In general inverse problem corresponds to estimation of parametric or non-parametric changes based on the knowledge assimilated in the forward problem and the observed time series data of quasi-stationary process response. The estimates of critical parameters can only be obtained within certain bounds at a particular confidence level. The online statistical information of the anomaly status is significant because it can facilitate early scheduling for the maintenance or repair of critical components or to prepare an advance itinerary of the damaged parts. The information can also be used to design control policies for damage mitigation and life extension. This chapter has addressed only the forward problem of detection of anomalous behavior and the inverse problem of parameter estimation is reported as an area of future work.

4.   Description of Experimental Apparatus

This section presents the description of the experimental apparatus that has been designed and fabricated specifically to study the characteristics of complex mechanical vibration systems that have the capacity of multiple degrees of freedom for motion along different coordinate directions. This special purpose experimental apparatus is shown in Figure 4. The experimental apparatus can be used to replicate the vibration response of a mechanical
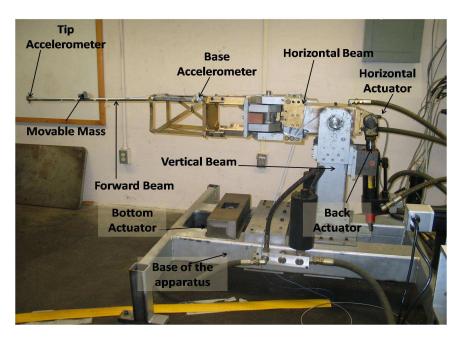
Figure 4. Multi-degree of freedom mechanical vibration apparatus

structure such as a support beam under external excitation (e.g. seismic). The apparatus has three principle degrees of freedom that arise from three actuators that provide the capability of motion along three different directions. Each of the actuator is excited using a remote computer through an electro-hydraulic position feedback control and is capable of providing a force up to 3,400 kgf. The actuators can be excited over a wide band of frequency range and can produce oscillations of significant magnitude.

The experimental apparatus consists of a rectangular base that is bolted to the ground and supports two beams - horizontal (B_h) and vertical (B_v), and three actuators - bottom (A_y), back (A_z) and horizontal (A_x). Figure 5 gives a two-dimensional schematic of the apparatus. The base of the vertical beam B_v is connected to the bottom actuator A_y that moves the vertical beam in the yz-plane about the hinge h_y. The back actuator A_z is mounted on the vertical beam and moves the horizontal beam B_h, pivoted at h_z, in the yz-plane. The horizontal actuator A_x rotates the test beam about the pivot point h_x in the xy-plane. Thus, the angular motion of the beams B_v and B_h about the hinges h_x, h_y and h_z are controlled by the linear motions of the three actuators A_x, A_y and A_z. For small angular displacements of the beams, their angular motions translate into the movement of the point P in three axes - x, y and z. The test beam is mounted at point P and it can be given a desired base excitation in all or any direction of motion. The structure of beams is made from 6mm thick hollow square steel sections.

The multi-degree of freedom mechanical vibration apparatus in Figure 4 is logically partitioned into two subsystems as described below.

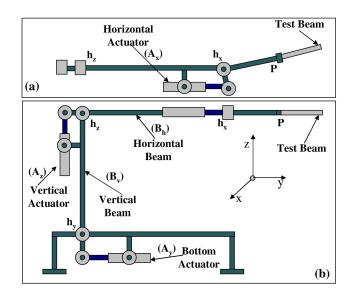a) *The plant subsystem* consists of the mechanical structure including flexible hinges

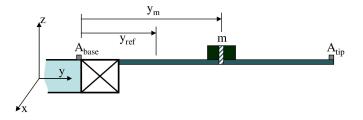Figure 5. 2-D schematic of the Multi-degree of freedom apparatus (a) Top View (b) Side View

Figure 6. Schematic of the test beam structure

that connect the beams, the hydraulic system, and the actuators and

b) *The control and instrumentation subsystem* consists of control computers, data acquisition and processing system, communications hardware and software, and the sensors. The sensors include: i) linear variable differential transformers ($LVDT$) for displacement measurement and b) integrated circuit-piezoelectric shear accelerometers that are used to measure the vibrations of the tip and the base of the horizontal beam (see Figure 6). The sensitivity of sensor is 2.727 mV/ms^{-2}. The control system and data acquisition software is executed under DSpace platform on the windows operating system. The feedback control system shown in Figure 7 is installed on a Pentium pc along with necessary A/D and D/A interface to the feedback amplifiers connected to the sensors and actuators of the test apparatus.
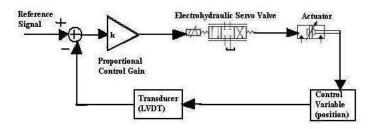
Figure 7. Control circuit for the mechanical vibration apparatus

4.1.   Hardware implementation and software structure

The multi-degree of freedom mechanical vibration apparatus (Figure 4) is interfaced with a DSpace Data Acquisition Board having 16 A/D channels and 8 D/A channels. Data acquisition is carried out with a sampling rate at 1 KHz for monitoring and control. The time series data for statistical pattern recognition can be decimated as required. The real-time instrumentation and control subsystem of this test apparatus is implemented on a Pentium PC platform. The software runs on the Windows XP Operating System and is provided with A/D and D/A interfaces to the amplifiers serving the sensors and actuators through the Control desk front end. The Control desk front end loads a Simulink (Matlab based) module on to the data acquisition card to perform real-time communication tasks, in addition to data acquisition and built-in tests (e.g., software limit checks and saturation checks).

4.2.   Experimental procedure

This section describes the experimental procedure to detect the parametric changes in the system. The horizontal beam as shown in Figure 4 and 5 has a slender test beam attached to it through an intermediate complex truss structure. The test beam has a length of 1150 mm. The test beam has a movable mass ($\sim$158 gm) attached to it that has the provision of being secured at different positions on the test beam. The schematic of this arrangement is shown in Figure 6. A change in the position of the mass on the test beam causes a change in the mass moment of inertia of the beam causing a change in the dynamics of the test system. Therefore, a change in the mass position affects the vibration response of the system. The apparatus is equipped with two accelerometers to measure the vibration response at the tip (A_{tip}) and the base (A_{base}) of the test beam as shown in Figure 6. In the current investigation, the parameter under consideration is the position of the mass and any change in this position is measured using the analysis of the time series data of two accelerometers.

The horizontal (A_x) and back (A_z) actuators are excited by a trapezoidal reference input of amplitude 2 V and frequency 6.35Hz as shown in Figure 8, while the bottom actuator A_y is held fixed. The trapezoidal input is achieved by a rectified sine wave. This excitation signal is generated in such a way that at any time instant at least one of the actuators is in motion and there is a phase difference between the two actuators A_x and A_z. This is done to ensure less power consumption from the hydraulic unit which helps to reduce the overheating of hydraulic fluids and reduce the noise. The same excitation signal is given
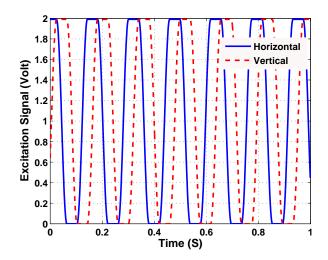
Figure 8. Excitation signal generation

to the closed loop plant for each position of the movable mass on the test beam and time series data from both accelerometers is recorded for 30 seconds after the system reaches its steady state. The sampling frequency is 1kHz to accurately measure the performance of the system under parametric changes. This experimental procedure is repeated for different positions of the mass on the test beam.

Each run of the experiment starts with the movable mass placed at a reference point (y_{ref}) that is fixed at a distance of 540 mm from the base of the test beam (see Figure 6). The mass is moved by a total of 125 mm towards the tip of the test beam in increments of 12.5 mm and the corresponding time series data is recorded. The set of time series data is used to measure anomaly (i.e., a change in the performance) in the system due to change in the mass position as compared to the reference condition.

5.   Results and Discussion

This section presents the results generated from different experiments conducted on the multi-degree of freedom mechanical vibration apparatus described in the previous section. The set of time series data generated for different positions of the mass from the two accelerometers was processed using the method of symbolic dynamic filtering (SDF) as described in Section 3.. Both accelerometers used in the experiment give the horizontal and vertical component of acceleration as V_x and V_z respectively. The resultant time-series obtained as $V_r = \sqrt{(V_x^2 + V_z^2)}$ has been used for further analysis. Time series data corresponding to the position of the mass at maximum distance from the reference (i.e., $y_m - y_{ref}$ = 125 mm) was used to create a partition for the analysis because the data displays maximum amplitude at this position. The partitioning was done using the Analytic Signal Space Partitioning ($ASSP$) [18] (see Section 3.), where the concept of maximum entropy parti-

tion was used to divide the Hilbert transformed data into $|\Sigma| = |\Sigma_R| \cdot |\Sigma_A| = 12$ cells such that $|\Sigma_R|$=4 and $|\Sigma_A|$=3. The depth of D-Markov machine was chosen to be D=1 for this analysis. Thus the number of states of the machine is the same as the alphabet size. The anomaly measure (Eq. 12) was computed for each position of the mass on the test beam. A non-zero anomaly measure indicates changes in the response of the sensors due to parametric changes relative to the nominal condition.

Figure 9 shows the results derived from time series data of the tip accelerometer (A_{tip}). The figure is divided into six subplots, where each subplot contains three figures - (i) the top figure showing the vertical component of tip acceleration with sensor output V_z in volts, (ii) the middle figure showing the horizontal component of tip acceleration with sensor output (V_x) in volts, and (iii) the bottom figure showing the probability distribution of different symbolic states (i.e., cells) along the radial and angular directions of the partition of the Hilbert transformed data. The probability distributions are derived from the resultant of the vertical (V_z) and horizontal (V_x) components of the data. Each subplot in Figure 9 corresponds to a different position of the movable mass m on the beam. The first subplot, i.e., case(a), corresponds to the nominal condition of system when the mass is placed at the reference position $y_m = y_{ref}$ on the test beam (see Figure 6). Each of the subsequent subplots, i.e., cases (b) to (f), corresponds to the mass position shifted by 25 mm towards the tip of the beam such that $y_m - y_{ref}$ =25, 50, 75, 100 and 125 mm, respectively.

As the mass is moved towards the tip of the test beam, the amplitude of time series data obtained from the tip accelerometer increases with increase in vibrations of the beam. When the distance of the mass from the reference position is small, the changes in the raw time series data cannot be directly detected by visual inspection of the data. This is evident from the plots of time series data in Figure 9 for cases (a), (b) and (c), that correspond to the position of the mass at $y_m - y_{ref}$= 0, 25 and 50 mm, respectively. However, the bar plots corresponding to each of these three cases show appreciable change in the probability distribution with respect to the nominal condition (i.e., case (a)). This indicates that the method of Symbolic Dynamic Filtering (SDF) is able to extract the embedded signatures of parametric changes in the system from the vibration characteristics of the accelerometer data. As the mass is moved further towards the tip, the changes in the vibration characteristics become more pronounced. This is reflected in drastic changes in the corresponding probability distribution plots. When the mass is moved to the maximum distance of approximately 125 mm, the probability distribution converges to uniform distribution of states indicating a high vibrating condition.

The probability distributions shown in Figure 9 contain the vibration characteristics of the system. The anomaly measure (Eq. 12) is computed to quantify the changes in the state probabilities as compared to the reference condition. This anomaly measure is then used to track the changes in the vibrations of the test beam with shifts in the position of the mass. The reference condition is chosen to be the mass position at $y_m = y_{ref}$ (i.e., case (a) in Figure 9). Plots of anomaly measure versus the position of the mass ($y_m - y_{ref}$) are shown in Figure 10 for the tip and the base sensors.
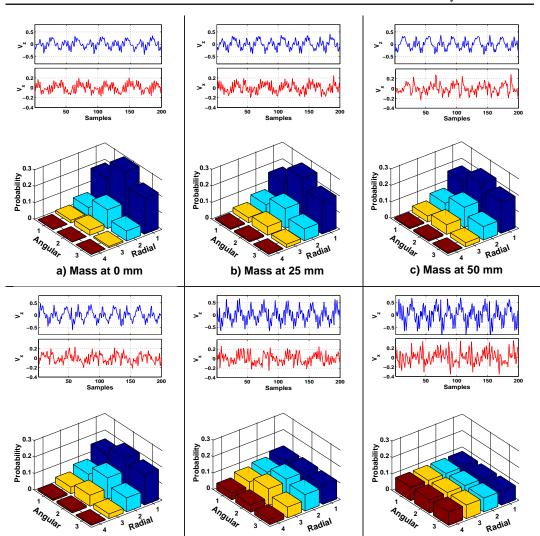
Figure 9. Vertical and horizontal component of tip accelerometer data and corresponding probability distribution of symbolic states derived from the resultant of the two components for different positions of mass. Case (a) nominal condition with Mass at Reference point, $y_m - y_{ref} = 0mm$, (b) $y_m - y_{ref} = 25mm$ (c) $y_m - y_{ref} = 50mm$ (d) $y_m - y_{ref} = 75mm$, (e) $y_m - y_{ref} = 100mm$ (f) $y_m - y_{ref} = 125mm$
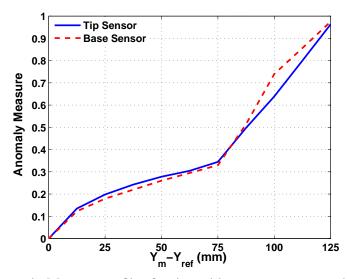
Figure 10. Anomaly Measure profiles for tip and base sensors versus the position of the mass $(y_m - y_{ref})$

Figure 10 shows the anomaly measure profiles derived from the time series data of the sensors mounted at the tip and the base of the test beam (see Figure 6). As the mass is moved from the reference point (y_{ref}) towards the tip of the beam, the mass moment of inertia of the beam changes causing a greater influence on the vibration characteristics of the beam. This trend is in agreement with the observation of the experimental data. It can be seen in the plots of Figure 10 that anomaly measure profiles of both the tip and the base sensors increase as the mass is moved away from the reference point towards the tip of the test beam. It is to be noted that anomaly measure is a relative measure and is computed with respect to the nominal condition $(y_m = y_{ref})$, therefore, it is not an indicative of the true position of the mass. A change in the value of anomaly measure indicates a parametric change in the system; however, estimation of such a change is the inverse problem [37].

For solution of the inverse problem multiple experiments need to be conducted under similar experimental conditions to generate sufficient statistical data. Variations among experiments conducted under (apparently) identical conditions are normally expected due to the uncertainties present in the system. These uncertainties are caused due to several factors such as: i) measurement noise, ii) errors in the positioning of the mass, and iii) small fluctuations in the excitation waveform caused by imprecisions in the electro-hydraulic and mechanical connections. Therefore anomaly measure profiles from different experiments may show similar trends but their profiles would not be exactly identical. As such, solution of the inverse problem for parameter estimation [37] is currently under investigation and would be reported in future publications.

6. Summary, Conclusions and Future Work

A vast majority of human-engineered complex systems are subjected to mechanical vibration, where a major goal is online detection and estimation of behavioral uncertainties due to gradual development of anomalies (i.e., deviations from the nominal condition). These anomalies (benign or malignant) may alter the quasi-static behavior of mechanical vibration mechanism that causes degradation of system performance and may eventually lead to widespread catastrophic failures. Since it is often infeasible to achieve the required modeling accuracy and precision in complex dynamical systems, time series analysis of appropriate sensor measurements provides one of the most powerful tools for degradation monitoring of complex vibration systems.

This chapter presents a recently reported technique of data-driven pattern recognition, called Symbolic Dynamic Filtering (SDF), for online detection and estimation of behavioral uncertainties due to slowly evolving anomalies. The underlying concept of SDF is built upon the principles of Statistical Mechanics, Symbolic Dynamics and Information Theory, where time series data from selected sensor(s) in the fast time scale of the process dynamics are analyzed at discrete epochs in the slow time scale of anomaly evolution. Symbolic dynamic filtering includes preprocessing of time series data using the Hilbert transform. The transformed data is partitioned using the maximum entropy principle. Subsequently, statistical patterns of evolving anomalies are identified from these symbolic sequences through construction of a (probabilistic) finite-state machine that captures the system behavior by means of information compression. The concept of SDF has been experimentally validated on a special-purpose computer-controlled multi-degree of freedom mechanical vibration apparatus that is instrumented with two accelerometers for identification of anomalous patterns due to parametric changes.

The work, reported in this chapter, is a step toward building a reliable instrumentation system for early detection of parametric and non-parametric changes (e.g., incipient faults) and prognosis of potential catastrophic failures. Further theoretical and experimental research is necessary before its usage in industry. The online information, provided by symbolic patterns that are derived from the sensor time series data, is useful for decision and control of human-engineered complex system to sustain order and normalcy under both anticipated and unanticipated faults and disturbances. In this context, solution of the inverse problem and development of performance bounds for safe reliable operation of different engineering applications is an active area of current research [37].

Acknowledgements

References

[1] S. Gupta, A. Ray, and E. Keller, "Symbolic time series analysis of ultrasonic data for early detection of fatigue damage," *Mechanical Systems and Signal Processing*, vol. 21, no. 2, pp. 866–884, 2007.

[2] S. Gupta, *Complex Systems in Engineering: A Symbolic Dynamics Approach for Anomaly Detection*. VDM-Verlag Publishers, Germany, ISBN 978-3-639-10105-8, 2008.

[3] E. Ott., *Chaos in Dynamical Systems*. Cambridge University Press, 1993.

[4] S. Ozekici, *Reliability and Maintenance of Complex Systems*, vol. 154. NATO Advanced Science Institutes (ASI) Series F: Computer and Systems Sciences, Berlin, Germany, 1996.

[5] A. Doucet, N. de Freitas, and N. Gordon, *Sequential Monte Carlo Methods in Practice*. Springer, New York, 2001.

[6] C. Andrieu, A. Doucet, S. Singh, and V. B. Tadic, "Particle methods for change detection, system identification, and control," *Proceedings IEEE*, vol. 92, no. 3, pp. 423–438, 2004.

[7] A. Ray, "Symbolic dynamic analysis of complex systems for anomaly detection," *Signal Processing*, vol. 84, no. 7, pp. 1115–1130, 2004.

[8] S. Gupta and A. Ray, *Symbolic Dynamic Filtering for Data-Driven Pattern Recognition*. Chapter 2 in Pattern Recognition: Theory and Application, Editor- E.A. Zoeller, Nova, Science Publisher, Hauppage, NY,USA, 2007.

[9] D. Lind and M. Marcus, *An Introduction to Symbolic Dynamics and Coding*. Cambridge University Press, United Kingdom, 1995.

[10] C. S. Daw, C. E. A. Finney, and E. R. Tracy, "A review of symbolic analysis of experimental data," *Review of Scientific Instruments*, vol. 74, no. 2, pp. 915–930, 2003.

[11] H. E. Hopcroft, R. Motwani, and J. D. Ullman, *Introduction to Automata Theory, Languages, and Computation, 2nd ed.* Addison Wesley, Boston, 2001.

[12] R. K. Pathria, *Statistical Mechanics*. Elsevier Science and Technology Books, 1996.

[13] S. Gupta, and A. Ray,"Statitical Mechanics of Complex Systems for Pattern Identification," *Journal of Statistical Physics*, vol. 134, no. 2, pp. 337-364, 2009.

[14] R. Badii and A. Politi, *Complexity hierarchical structures and scaling in physics*. Cambridge University Press, United Kingdom, 1997.

[15] C. Beck and F. Schlögl, *Thermodynamics of chaotic systems: an introduction.* Cambridge University Press, United Kingdom, 1993.

[16] M. Buhl and M. Kennel *Phys. Rev. E*, vol. 71, 046213, 2005.

[17] V. Rajagopalan and A. Ray, "Symbolic time series analysis via wavelet-based partitioning," *Signal Processing*, vol. 86, no. 11, pp. 3309–3320, 2006.

[18] A. Subbu and A. Ray, "Space partitioning via hilbert transform for symbolic time series analysis," *Applied Physics Letters*, vol. 92, p. 084107, February 2008.

[19] W. J. Wang, Z. T. Wu, and J. Chen, "Fault identification in rotating machinery using the correlation dimension and bispectra," *Nonlinear Dynamics*, vol. 25, pp. 383–393, August 2001.

[20] C. N. M. S. S. T. M. T. L. P. L. Moniz, J.M. Nichols and L. Virgin, "A multivariate, attractor-based approach to structural health monitoring," *Journal of Sound and Vibration*, vol. 283, pp. 295–310, May 2005.

[21] P. D. McFadden, "Detection of gear faults by decomposition of matched differences of vibration signals," *Mechanical Systems and Signal Processing*, vol. 14, pp. 805–817, Sept. 2000.

[22] M. R. Dellomo, "Helicopter gearbox fault detection: A neural network based approach," *Journal of Vibration and Acoustics*, vol. 121, no. 3, pp. 265–272, 1999.

[23] Z. K. Peng, P. W. Tse, and F. L. Chu, "A comparison study of improved hilbert-huang transform and wavelet transform: Application to fault diagnosis for rolling bearing," *Mechanical Systems and Signal Processing*, vol. 19, pp. 974–988, Sept. 2005.

[24] H. Ocak and K. A. Loparo, "Estimation of the running speed and bearing defect frequencies of an induction motor from vibration data," *Mechanical Systems and Signal Processing*, vol. 18, pp. 515–533, May 2004.

[25] H. Sohn, J. A. Czarnecki, and C. R. Farrar, "Structural health monitoring using statistical process control," *Journal of Structural Engineering*, vol. 126, no. 11, pp. 1356–1363, 2000.

[26] J. Sakellariou and S. Fassois, "Vibration based fault detection and identification in an aircraft skeleton structure via a stochastic functional model based method," *Mechanical Systems and Signal Processing*, vol. 22, pp. 557–573, April 2008.

[27] C. Kar and A. Mohanty, "Vibration and current transient monitoring for gearbox fault detection using multiresolution fourier transform," *Journal of Sound and Vibration*, vol. 311, pp. 109–132, March 2008.

[28] Z. K. Peng, P. W. Tse, and F. L. Chu, "An improved hilbert-huang transform and its application in vibration signal analysis," *Journal of Sound and Vibration*, vol. 286, pp. 187–205, August 2005.

[29] H. Ocak and K. A. Loparo, "Hmm-based fault detection and diagnosis scheme for rolling element bearings," *Journal of Vibration and Acoustics*, vol. 127, no. 4, pp. 299–306, 2005.

[30] J. Sanz, R. Perera, and C. Huerta, "Fault diagnosis of rotating machinery based on auto-associative neural networks and wavelet transforms," *Journal of Sound and Vibration*, vol. 302, pp. 981–999, May 2007.

[31] X. Lou and K. A. Loparo, "Bearing fault diagnosis based on wavelet transform and fuzzy interference," *Mechanical Systems and Signal Processing*, vol. 18, pp. 1077–1095, 2004.

[32] B. I. Epureanu, L. S. Tang, and M. P. Païdoussis, "Exploiting chaotic dynamics for detecting parametric variations in aeroelastic systems," *AIAA Journal*, vol. 42, pp. 728–735, April 2004.

[33] D. Chelize and J. P. Cusumano, "A dynamical systems approach to failure prognosis," *Journal of Vibration and Acoustics*, vol. 126, pp. 2–8, January 2004.

[34] J. M. Nichols, M. Seaver, S. T. Trickey, M. D. Todd, C. Olson, and L. Overbey, "Detecting nonlinearity in structural systems using the transfer entropy," *Physical Review E (Statistical, Nonlinear, and Soft Matter Physics)*, vol. 72, no. 4, p. 046217, 2005.

[35] S. Chin, A. Ray, and V. Rajagopalan, "Symbolic time series analysis for anomaly detection: A comparative evaluation," no. 9, pp. 1859–1868, September 2005.

[36] S. Gupta, A. Ray, and E. Keller, "Fatigue damage monitoring by ultrasonic measurements: A symbolic dynamics approach," *International Journal of Fatigue*, vol. 29, no. 6, pp. 1100–1114, 2007.

[37] S. Gupta and A. Ray, "Real-time fatigue life estimation in mechanical systems," *Measurement Science and Technology*, vol. 18, no. 7, pp. 1947–1957, 2007.

[38] A. Khatkhate, A. Ray, E. E. Keller, S. Gupta, and S. Chin, "Symbolic time series analysis for anomaly detection in mechanical systems," *IEEE/ASME Trans. on Mechatronics*, vol. 11, no. 4, pp. 439–447, 2006.

[39] S. Chakraborthy, S. Sarkar, S. Gupta and A. Ray, "Damage Monitoring of Refractory Wall in a Generic Entrained-bed Slagging Gasification System," *Proceedings of the Institution of Mechanical Engineers: Part A- Journal of Power and Energy*, vol. 222, no. 8, pp. 791-807, 2008.

[40] S. Gupta, A. Ray, and A. Mukhopadhyay, "Anomaly detection in thermal pulse combustors using symbolic time series analysis," *Proceedings of the Institution of Mechanical Engineers- Part I- Journal of Systems and Control Engineering*, vol. 220, no. 5, pp. 137–146, 2006.

[41] A. Khatkhate, S. Gupta, A. Ray, and R. Patankar, "Anomaly detection in flexible mechanical couplings via symbolic time series analysis," *Journal of Sound and Vibration*, vol. 311, no. 3-5, pp. 608–622, 2008.

[42] S. Gupta and A. Ray, "Pattern identification using lattice spin systems: A thermodynamic formalism," *Applied Physics Letters*, vol. 91, no. 19, p. 194105, 2007.

[43] H. Kantz and T. Schreiber, *Nonlinear Time Series Analysis, 2nd ed.* Cambridge University Press, United Kingdom, 2004.

[44] S. Mallat, *A Wavelet Tour of Signal Processing 2/e.* Academic Press, 1998.

[45] D. Gabor *Journal of Communication Engineering*, vol. 93, 429, 1946.

[46] L. Cohen, P. Loughlin, and D. Vakman *Signal Processing*, vol. 79, 301, 1999.

[47] T. M. Cover and J. A. Thomas, *Elements of Information Theory*. John Wiley, New York, 1991.

[48] R. B. Bapat and T. E. S. Raghavan, *Nonnegative Matrices and Applications*. Cambridge University Press, 1997.

[49] A. Tarantola, *Inverse Problem Theory*. Society for Industrial and Applied Mathematics, 2005.

[50] K. Sobczyk and B. F. Spencer, *Random Fatigue: Data to Theory*. Academic Press, Boston, MA, 1992.